Fuel 109 (2013) 125–136

Contents lists available at SciVerse ScienceDirect

Fuel

journal homepage: www.elsevier.com/locate/fuel

The combustion properties of 1,3,5-trimethylbenzene and a kinetic model

Pascal Diévart [a], Hwan Ho Kim [a], Sang Hee Won [a], Yiguang Ju [a], Frederick L. Dryer [a], Stephen Dooley [a,b,*], Weijing Wang [c], Matthew A. Oehlschlaeger [c]

[a] Department of Mechanical and Aerospace Engineering, Princeton University, Princeton, NJ, United States
[b] Department of Chemical and Environmental Sciences, University of Limerick, Limerick, Ireland
[c] Department of Mechanical, Aerospace and Nuclear Engineering, Rensselaer Polytechnic Institute, Troy, NY, United States

HIGHLIGHTS

- 1,3,5-trimethylbenzene is a proposed surrogate fuel component for jet aviation fuels.
- Ignition delay times and laminar burning velocities of 1,3,5-trimethylbenzene are presented.
- Constant pressure reactivity profiles show no reactivity at less than 930 K.
- Kinetic models for 1,3,5-trimethylbenzene combustion are constructed and tested.
- Model analysis offers a proposition of the 1,3,5-trimethylbenzene combustion mechanism

ARTICLE INFO

Article history:
Received 29 September 2012
Received in revised form 20 November 2012
Accepted 22 November 2012
Available online 25 December 2012

Keywords:
Aromatic hydrocarbon
1,3,5-Trimethylbenzene
Ignition delay
Flame properties
Combustion model

ABSTRACT

Trimethylbenzenes have been suggested as useful components for the formulation of simple hydrocarbon mixtures that quantitatively emulate the gas-phase combustion behaviour of real liquid transportation fuels as model or surrogate fuels. To facilitate this application, various combustion properties of 1,3,5-trimethylbenzene (mesitylene) have been characterised experimentally and a new chemical kinetic model for its combustion constructed. Experimental determinations of 1,3,5-trimethylbenzene reflected shock ignition delay, laminar burning velocities and high-pressure flow reactor oxidative reactivity profiles are presented. These data allow for the testing of a detailed kinetic model, developed by direct analogy to, and incorporating as a subcomponent, a recent comprehensively tested kinetic model for toluene oxidation [Metcalfe WK, Dooley S, Dryer FL. Energy Fuels 2011; 25: 4915–4936]. Model calculations are also compared against data pertinent to 1,3,5-trimethylbenzene combustion phenomena from the published literature. The modelling approach allows for the accurate reproduction of the global combustion phenomena of ignition delay, burning velocity, diffusive and premixed strained extinction limits and flow reactor reactivity, with some noted shortcomings. Analyses of the constructed model suggest that the mechanism of 1,3,5-trimethylbenzene combustion occurs through the formation of 3,5-dimethylbenzaldehyde and 1,2-bis(3,5-dimethylphenyl) ethane as the major stable intermediate species, with relative proportions depending on the conditions of the particular reacting environment.

1. Introduction

Aromatic hydrocarbons are major components of fossil-derived transportation fuels. Their combustion properties are distinct from those of other fossil fuel constituents, for example normal-alkanes, as they have a propensity to generate relatively stable intermediate radical species. Thus, the presence of aromatic species inhibits the oxidative reactivity of alkane/aromatic mixtures relative to that of pure alkanes, e.g. [1–2]. The aromatic components of liquid fuels are also known to be important contributors to the formation of the polyaromatic hydrocarbons (PAHs) that are soot precursors.

Therefore, aromatic components appear a necessary constituent of surrogate mixture formulations that aspire to emulate some combustion behaviour of real fossil-derived liquid transportation fuels. Recently, a methodology for the formulation of surrogate (or model) fuels for liquid transportation fuels has been proposed and tested for the specific example of aviation fuels [5–7]. The sharing of four key fuel properties in Hydrogen-to-Carbon molar ratio (H/C), Derived Cetane Number (DCN), Threshold Sooting Index (TSI) and Average Molecular Weight (MW_{ave}), in addition

* Corresponding author at: Department of Chemical and Environmental Sciences, University of Limerick, Limerick, Ireland. Tel.: +353 61 234628.
E-mail address: stephen.dooley@ul.ie (S. Dooley).

0016-2361/$ - see front matter © 2012 Elsevier Ltd. All rights reserved.
http://dx.doi.org/10.1016/j.fuel.2012.11.069

to the provision of the important chemical functional groups, allows for the reactivity of a surrogate fuel to be regulated to that of a specific target real fuel with quantitative fidelity [5–7]. Toluene was utilised as a surrogate mixture component in the earlier provisional formulation [5] which concentrated on premixed chemical kinetic dominated combustion phenomena. At that time it was recognised that the specific components utilised, particularly toluene, would not be suitable for emulating the diffusive and sooting nature of gas turbine fuels simultaneously. In subsequent work [6], two larger alkyl aromatic isomers, n-propylbenzene and 1,3,5-trimethylbenzene, were utilised in combination as the aromatic surrogate components in order to increase the average molecular weight of the model fuel and to provide further independent control of the oxidative reactivity (DCN) and sooting propensity (TSI) parameters. The preference of 1,3,5-trimethylbenzene (mesitylene) over other trimethylbenzene isomers is due to the symmetry of the molecule, which allows for an assumed simplification of combustion model development.

Toluene, the simplest alkyl aromatic, is present in substantial quantities in gasoline, and has been utilised frequently as a model aromatic structure, e.g. [3–5]. Numerous experimental and computationally efforts (e.g. [8–23]) have been made to qualitatively and quantitatively understand its pyrolysis and oxidation chemistry and thermodynamics, though there still remains important inconsistencies and uncertainties in the understanding of the same [21].

By comparison, experimental and modelling studies on poly methylated aromatics are relatively scarce, and have mainly focused on the dimethylbenzene (xylene) isomers. Gail et al. [24–26] have published speciation profiles for ortha-, meta- and para-xylene (high-pressure oxidation in a jet stirred reactor). Gudiyella et al. [27] conducted speciation measurements during the high temperature m-xylene ignition delay in a single-pulse shock tube. Battin-Leclerc et al. [28], Shen et al. [29], and Roubaud et al. [30] have performed ignition delay measurements of the xylenes in shock tubes and a rapid compression machine respectively. In these works, kinetic models were also proposed and tested against the different sets of experimental data [24–28]. For the trimethylbenzene isomers, Won et al. [31] have determined the extinction limits of 1,3,5-trimethylbenzene/air diffusion flames, Ji et al. [32] and Farrell et al. [33] have measured laminar burning velocities of premixed 1,3,5-trimethylbenzene/air flames as Hui et al. [34] also recently reported, in addition to premixed extinction limits of 1,3,5-trimethylbenzene/O_2/N_2 mixtures. The 1,2,4-trimethyl benzene isomer has also received some attention, being considered in an aviation fuel surrogate composition with n-decane by Honnet et al. [35]. For this isomer, pure component data sets are available from Roubaud et al. [30], Won et al. [31], Ji et al. [32], and Hui et al. [34] for rapid compression machine ignition delay [30], diffusion flame extinction [31,32], premixed flame extinction [34], and laminar burning velocity respectively [32,34].

It appears that the use of heavier alkyl benzenes such as 1,3,5-trimethylbenzene are required for surrogate fuel formulations for aviation gas turbine and diesel type fuels [5,6,36]. Thus, this study aims to extend the experimental database for 1,3,5-trimethylbenzene combustion model development and testing through measurement of ignition delay times, laminar flame velocities, and speciation profiles in a flow reactor. A previously described toluene model [21] which substantially incorporates the available literature knowledge of fundamental and observational nature is employed as a template for the construction and development of an original model for the combustion kinetics of 1,3,5-trimethylbenzene. The experimental data presented here and the appropriate previously reported literature data are used to test the model. The paper then presents a short analysis of the combustion oxidation mechanism of 1,3,5-trimethylbenzene as suggested by the kinetic model in terms of the requirement for remaining developmental needs.

2. Experimental

2.1. Shock tube ignition delay

Ignition delay measurements are performed in a heated high-pressure shock tube (5.7 cm inner diameter) at *Rensselaer Polytechnic Institute* that has been previously described [15,29]. The whole facility is maintained at 403 K (130 °C), a temperature sufficiently high to ensure the full vaporisation of the test mixtures. Three fuel/air mixtures, of equivalence ratio 0.5, 1.0 and 2.0 are studied, the mole fraction compositions of which are provided in Table 1. Throughout this study, equivalence ratio (Φ) is defined as the ratio of fuel to air to achieve stoichiometric combustion (unity). The mixtures are prepared by direct injection of a measured mass of liquid fuel into a similarly heated mixing vessel. After vaporisation of the 1,3,5-trimethylbenzene fraction (98 + % purity), N_2 (99.995% purity), and O_2 (99.995% purity) are added to achieve the desired final mixture composition. Mixture mole fractions are determined manometrically and the mixtures are mechanically mixed with a rotating vane assembly for 20 min to 4 h prior to the experiments. Confirmation of reactant mixture composition and the stability of heated reactant mixtures have been previously carried out for multi-component hydrocarbon fuel/air and alkyl ester/air mixtures through gas chromatographic analyses of test mixtures after both preparation and loading into the shock tube. Given that 1,3,5-trimethylbenzene is more stable than normal-paraffinic and ester containing fuels, it may be safely assumed that the reactant mixtures are stable and their composition is as specified via partial pressures. Post-shock conditions are determined through the normal shock relations utilising measurements of incident shock velocity, initial temperature and pressure, and the thermodynamic properties of the reacting mixture [29] which are described in the kinetic modelling section of this paper. The ignition delay time is defined as the time interval between the shock arrival/reflection at the end wall and the onset of ignition as apparent by measurement of electronically-excited OH chemiluminescence observed at the end wall. The uncertainty in the determined reflected shock temperature and pressure is estimated to be less than 1.5% and 2% respectively of the nominal value. Considering contributions from uncertainties in reflected shock conditions and uncertainties due to interpretation of measured pressure and chemiluminescence signals, the worst case estimated uncertainty in reported ignition delay times is ±25%, displayed representatively in Fig. 2.

2.2. Spherical bomb laminar burning velocity

This experimental setup at *Princeton University* is composed of a spherical combustion bomb operated under nearly constant pressure, fuel vaporisation chamber, oven, and pressure release system as described thoroughly by Kim et al. [37]. The spherical bomb has a 20 cm inner diameter. Two 250 μm diameter tungsten electrodes are installed at the top and bottom of the bomb and the upper electrode is mounted with a linear motion device to control the separation distance between the electrodes. The bomb is housed inside of an oven heated by two electrical heaters (total 2200 W) with an electric fan to achieve a uniform temperature distribution. K-type thermocouples are installed at the top and bottom of the oven to

Table 1
Mixture mole fractions and fuel/oxygen equivalence ratio, Φ, for shock tube study.

Mixture	1,3,5-Trimethylbenzene	O_2	N_2
Φ = 1.0 in air	0.0187	0.2061	0.7752
Φ = 0.5 in air	0.0095	0.2080	0.7825
Φ = 2.0 in air	0.0368	0.2023	0.7609

monitor temperature uniformity. The temperature inside the bomb is maintained at 400 K by PID control and a third K-type thermocouple located inside the combustion chamber. The inlet lines and vaporisation chamber are also heated to the same temperature as the oven.

The bomb is filled with a combustible mixture by the partial pressure method. 1,3,5-Trimethylbenzene (99% purity) is pre vaporised in a vaporisation chamber (500 cm^3) before being allowed to fill the bomb volume. Nitrogen (99.9%) and oxygen (99.5%) are subsequently added to the bomb through heated transfer lines. Following spark ignition generated by the tungsten electrodes, flame propagation is visualised using a high speed Schlieren imaging system [38]. To avoid the compression effect [38], only experimental data for flame radii less than 2.5 cm are used as the pressure inside of the bomb rises by less than 3% when a flame radius reaches 2.5 cm, which is the upper limit of all flames analysed in this study. Therefore, the near constant pressure assumption can be applied [38,39]. The unstretched burned flame speed is extracted from the linear relationship between burned flame speed and stretch rate, $K = (2/R_f) \times (dR_f/dt)$, where R_f is the flame radius and t, time. The laminar flame speed, S_u^0, is found by using the calculated equilibrium density ratio by linear extrapolation to zero stretch. Confinement effects are neglected because of the large inner diameter of the spherical bomb. As only data with a flame radius smaller than 25% of the spherical bomb radius are used in the evaluation of flame speed and stretch rate, no flow corrections are required due to compression effects caused by flame fronts in close proximity to the chamber wall [40]. Experimental reproducibility and repeatability determined from multiple tests at the same nominal experimental conditions have been established. In addition, experimental uncertainties have been analysed considering uncertainties and fluctuations in the measurement of pressure, temperature, mixture fraction, high-speed visualisation, and in data analysis. Uncertainties from the Schlieren system are negligible because of the high speed acquisition (15,000 fps) and high spatial resolution (86 pixel/cm). In a previous study of n-decane/air mixtures at the conditions utilised here [37], decomposition of the reactants due to vaporisation was tested for by gas chromatographic analysis of gas samples extracted from the bomb before ignition. For the case of n-decane, no decomposition or oxidation products were observed. Considering that 1,3,5-trimethylbenzene is much less reactive than n-decane, it is reasonable to assume that appreciable degradation of the intended reactants is not possible for the experimental conditions of this study. The overall uncertainty in laminar flame speed determination including all of the above is estimated to be 1.1–7.3% of the nominal value depending on the condition studied as shown in Fig. 4.

2.3. Variable Pressure Flow Reactor (VPFR) measurements

The design, instrumentation, and experimental methodology of the variable pressure flow reactor at *Princeton University* have been discussed in detail previously [41,42]. Arranged in a sequential flow-through configuration, the analytical instruments used to make the measurements reported here are a Fourier Transform Infrared (FTIR) spectrometer for water and 1,3,5-trimethylbenzene, an electrochemical oxygen analyser (O_2), and non-dispersive infrared analysers for carbon monoxide (CO) and carbon dioxide (CO_2). In the current study this device is operated at constant pressure (12.5 atm, where 1 atm is 1.013×10^5 Pa), constant residence time (1.8 s) and at variable reactor temperatures of 600–1000 K. A mass flow of 1,3,5-trimethylbenzene equating to 1 mole% carbon is delivered by a volumetric syringe pump and an oxygen mass flow equating to 0.447 mole% is prescribed to produce a stoichiometric fuel dilute mixture in nitrogen. The use of dilute conditions restricts axial concentration and thermal gradients within the reactor such that diffusive effects are small relative to convective effects and local and total heat release do not depart from the reactor initial gas temperature when matched by the reactor wall temperatures by more than 80 K; thus adiabatic reaction conditions are approximated.

The inert nature of the 1,3,5-trimethylbenzene/oxygen mixtures at the temperatures of the various vaporisation apparatuses employed in this study is confirmed by these flow reactor tests. 1,3,5-Trimethylbenzene is observed by infra-red spectroscopy to be stable in the presence of oxygen at temperatures less than ~670 K, even at timescales (1.8 s) and pressures (12.5 atm) much greater than encountered in the vaporisation apparatuses utilised in this study.

The uncertainties in the reported flow reactor measurements are $O_2 \leqslant 4\%$; $H_2O \leqslant 5\%$; $CO \leqslant 3\%$; and $CO_2 \leqslant 3\%$ (no less than 30 ppm), 1,3,5-trimethylbenzene $\leqslant 5\%$, of the reported reading. Other estimated measurement uncertainties are ±6 K in reported absolute temperatures (relative uncertainties are ±1.5 K), ±0.2 atm in reported pressures and ±0.04 s in the intended residence time of 1.8 s. These uncertainties are indicated as possible by representative uncertainty bars in Fig. 6.

3. Combustion model construction

A recently developed, extensively tested detailed chemical kinetic model for toluene oxidation [21], including C_1–C_4 and H_2/O_2 reaction sets, is utilised as the submodel for the current study. With the exception of information on the reaction of 1,3,5-trimethylbenzene with the hydroxyl radical [43–47], there is a paucity of fundamental information on the pyrolysis and oxidation reaction kinetics of 1,3,5-trimethylbenzene [48–50]. Given this situation, the 1,3,5-trimethylbenzene chemistry submodel is developed based upon analogy of local reaction centres to those of similar local thermochemical environments in the better studied toluene system as described by the Metcalfe et al. toluene submodel [21]. Where a thermochemical similarity in reaction centres is demonstrated, elementary reaction rate constants for the 1,3,5-trimethylbenzene oxidation system are prescribed as per the analogous rate constant proposed for toluene, modified to account for differences in degeneracy of the relative number of specific reaction sites, where appropriate. In all cases, reverse rate constants are inclusive of the 1,3,5-trimethylbenzene thermochemical parameters described in the following section. The species produced by the initial hydrogen abstractions from and decomposition reactions of 1,3,5-trimethylbenzene are mainly radicals found in the m-xylene (1,3-dimethyl benzene) oxidation system. Thus, an oxidation submodel for m-xylene was assembled from the works of Battin-Leclerc et al. [28] and Gail et al. [26] who have previously examined the reaction kinetics of this system.

3.1. Thermochemistry

The necessary thermochemical properties, C_P, ΔH_f, ΔS_f, etc. for all of the species considered in the 1,3,5-trimethylbenzene submodel are estimated using the group additivity method of Benson [51], where group contributions and corrections are consistent with the thermochemical database of the toluene submodel. These estimates for selected important species are compared to the available literature data [52–54] in Table 3. The resulting Bond Dissociation Energies (BDEs) on which rate constant prescriptions are based are also compared for the 1,3,5-trimethylbenzene and toluene systems. From Table 3 it can be seen that all recommendations for the enthalpy of formation (always at 298.15 K) of 1,3,5-trimethylbenzene are in close agreement at −3.7 to −3.8 kcal/mol, including the value proposed by Draeger (−3.8 kcal/mol) [54]. Similarly

Table 2
Reflected shock conditions and measured ignition delay times for shock tube study.

p (atm)	T (K)	1000/T (K^{-1})	t (μs)
Φ = 1.0 in air			
19.7	1134	0.8818	1123
21.7	1135	0.8811	1233
19.1	1169	0.8554	810
20.7	1170	0.8547	812
20.1	1171	0.8540	813
19.5	1182	0.8460	738
21.1	1185	0.8439	719
22.6	1203	0.8313	554
20.5	1251	0.7994	381
21.8	1302	0.7680	222
20.4	1305	0.7663	217
20.1	1334	0.7496	151
11.1	1135	0.8811	1733
11.3	1217	0.8217	832
10.7	1244	0.8039	565
10.6	1308	0.7645	295
10.1	1338	0.7474	192
10.2	1447	0.6911	74
Φ = 0.5 in air			
18.1	1166	0.8576	1009
21.6	1173	0.8525	858
21.3	1185	0.8439	830
21.8	1199	0.8340	789
20.3	1259	0.7943	376
20.7	1328	0.7530	179
20.1	1352	0.7396	143
21.1	1441	0.6940	59
10.1	1232	0.8117	640
10.3	1237	0.8084	732
10.4	1277	0.7831	448
11	1308	0.7645	311
9.8	1344	0.7440	183
10.3	1468	0.6812	69
Φ = 2.0 in air			
21.2	1111	0.9001	1055
21.5	1130	0.8850	904
19.8	1156	0.8651	655
19.9	1178	0.8489	502
20.5	1208	0.8278	381
19.2	1242	0.8052	281
20.7	1243	0.8045	262
19.8	1252	0.7987	230
19.4	1280	0.7813	205
19.1	1317	0.7593	155
12.2	1148	0.8711	963
10.9	1218	0.8210	471
10.6	1277	0.7831	255
10.1	1349	0.7413	101
10.7	1357	0.7369	96

Table 3
Enthalpies of formation (ΔH_f, kcal/mol) for 1,3,5-trimethylbenzene, toluene, relevant radical species and resulting Bond Dissociation Energies (BDEs, kcal/mol) at 298.15 K. See Fig. 1 for nomenclature. ‡ This study.

Species	ΔH_f (‡, [21])	ΔH_f [52]	ΔH_f [53]
$C_6H_5CH_3$	11.95	12.05	12.10
$1,3,5(CH_3)_3C_6H_3$	−3.8	−3.8	−3.7
$C_6H_5CH_2$	49.7	n/a	49.8
$3,5(CH_3)_2C_6H_3CH_2$	33.9	31.94	n/a
$(CH_3)C_6H_4$	72.7	71.80	n/a
$1,3,5(CH_3)_3C_6H_2$	56.9	56.62	n/a
H	52.1	n/a	52.1
CH_3	34.8	n/a	35.1
C_6H_5	81.2	n/a	80.7
$(CH_3)_2C_6H_3$	4.1	n/a	n/a
Bond	BDE (‡, [21])	Bond	BDE (‡, [21])
$(CH_3)_2C_6H_3CH_2$–H	89.9	$C_6H_5CH_2$–H	89.9
$(CH_3)_2C_6H_3$–CH_3	103.7	C_6H_5–CH_3	104.1
$(CH_3)_3C_6H_2$–H	112.9	$(CH_3)C_6H_4$–H	112.9

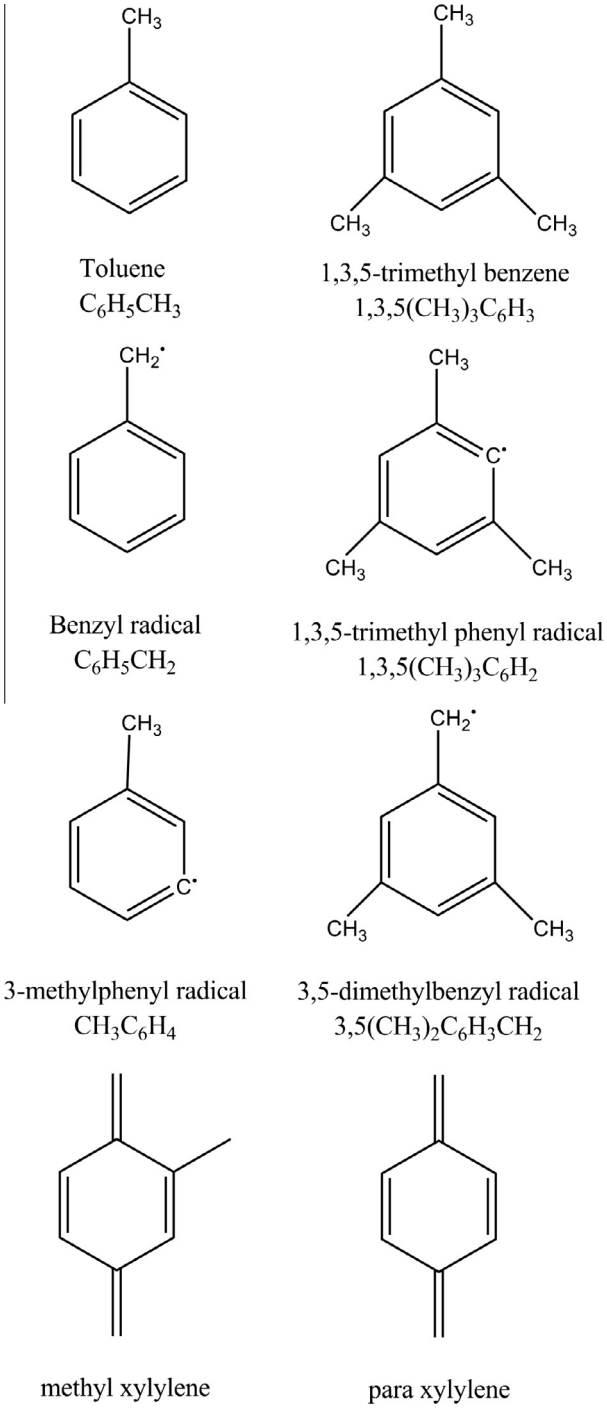

Fig. 1. Molecular structure and nomenclature of molecules and radicals referred to in text and in Table 1.

the suggested enthalpies of formation for the important fuel type radicals are in relatively close agreement, deviating by at most ~2 kcal/mol for the case of the 3,5-dimethylbenzyl radical ($(CH_3)_2C_6H_3CH_2$). Thus the reliability of the group additivity scheme in [21] for the generation of thermodynamic parameters has been assessed. It is noted that literature data specific to the trimethylbenzene oxidation systems is rather limited, as such, this is obviously a source of uncertainty in the kinetic model. Also shown in Table 3 are the bond dissociation energies resulting from these thermochemical estimates for the 1,3,5-trimethylbenzene and toluene systems. Equivalent positions in each molecule share similar BDEs,

thus the use of thermochemical kinetic analogies from one system to the other is supported [51].

3.2. Mass transport parameters

A Lennard-Jones collisional model is utilised to estimate binary diffusion coefficients of the chemical reaction model. The necessary Lennard-Jones parameters are estimated through the principle of corresponding states [55] when the required data are available (e.g. [56]), and are alternatively estimated using the correlations previously proposed by Dooley et al. [57].

3.3. 1,3,5-Trimethylbenzene chemical reaction pathways and rate constants

Temperature dependent reaction rate constants are defined in the model with use of the modified Arrhenius equation,

$$k = A \cdot T^{n} \cdot \mathrm{Exp}^{(-E_a/RT)}$$

where A, is the frequency factor of the reaction in question, T, the temperature, E_a, the activation energy and R, the Universal Gas Constant. This paper uses the default units of the chemkin solver, rate coefficients expressed in units of $cm^3\ mole^{-1}\ s^{-1}$, temperature in K and energy in calories.

Elementary reaction pathways are assigned to the 1,3,5-trimethylbenzene kinetic model by considering each of those presented by Metcalfe et al. [21] for the case of toluene oxidation, as described by the general classifications below.

3.3.1. Unimolecular fuel decomposition

Homolytic fission is considered for the methyl and phenylic C–H bonds as well as for the phenylic C–C bonds. The high-pressure limit rate constant for these reactions is estimated on a per carbon atom basis in the reverse recombination direction at a rate constant of $1.00 \times 10^{14} \times T^{0.0} \times \mathrm{Exp}\left(\frac{0\ \mathrm{cal/mol}}{RT}\right)\ \mathrm{cm^3\ mol^{-1}\ s^{-1}}$ for the recombination involving H atom and the phenylic radical. A rate constant of $7.22 \times 10^{13} \times T^{0.062} \times \mathrm{Exp}\left(\frac{44\ \mathrm{cal/mol}}{RT}\right)\ \mathrm{cm^3\ mol^{-1}\ s^{-1}}$ is prescribed for the recombination involving H atom and the benzylic type radical [21] ($1.10 \times 10^{14}\ \mathrm{cm^3\ mol^{-1}\ s^{-1}}$ at 1200 K), and a value of $2.33 \times 10^{14} \times T^{-0.283} \times \mathrm{Exp}\left(\frac{-191\mathrm{cal/mol}}{RT}\right)\ \mathrm{cm^3\ mol^{-1}\ s^{-1}}$ for methyl radical recombination with the phenylic type radical. These assignments are consistent with the equivalent theoretical recommendations of Klippenstein et al. [19] and Harding et al. [22] for the toluene system (e.g. $1.12 \times 10^{14}\ \mathrm{cm^3\ mol^{-1}\ s^{-1}}$ at 1200 K for benzyl radical + H atom ↔ toluene) and thus with the prescriptions of Metcalfe et al. [21] which are also very similar to those of Bounaceur et al. [58] for the toluene system.

The forward rate constant is computed from thermochemistry [51] and its pressure dependence subsequently estimated with the use of quantum Rice–Ramsperger–Kassel (QRRK) theory as described by Chang et al. [59] and Sheng et al. [60] using the collisional deactivation energy of $350 \times (T\ (\mathrm{K})/298\ \mathrm{K})^{0.30}\ \mathrm{cm^{-1}}$ ($[1.99 \times 10^{-28} \times (T\ (\mathrm{K})/298\ \mathrm{K})^{0.30}\ \mathrm{J}]$) (utilised in the work of Klippenstein et al. [19]).

3.3.2. Hydrogen abstraction

Hydrogen abstraction from 1,3,5-trimethylbenzene is considered from both benzylic and phenylic C–H bonds described by the rate constant prescriptions of Metcalfe et al. for the equivalent positions in the toluene system [21]. More specifically, the abstracting species considered are O_2, H, OH, O, HO_2, HCO, CH_3, C_2H_3, C_5H_5, C_6H_5, C_6H_5O as well as the isomers of C_3H_5, C_4H_5 and a number of large molecular weight fuel type radicals.

3.3.3. Ring substitution by H and O atoms and OH radicals

Methyl group substitution by H atoms is considered at the rate constant recommended by Ellis et al. [61,21] for the toluene system but modified to account for the degeneracy of methyl groups in the case of 1,3,5-trimethylbenzene ($2.85 \times 10^{6} \times T^{2.0} \times \mathrm{Exp}\left(\frac{-944\ \mathrm{cal/mol}}{RT}\right)\ \mathrm{cm^3\ mol^{-1}\ s^{-1}}$). Substitution of the 1,3,5-trimethylbenzene phenylic H atoms by O atom and OH radical is considered at rate constants of $8.0 \times 10^{12} \times T^{0.0} \times \mathrm{Exp}\left(\frac{-3600\ \mathrm{cal/mol}}{RT}\right)\ \mathrm{cm^3\ mol^{-1}\ s^{-1}}$ as prescribed by Bounaceur et al. [58] and $6.6 \times 10^{1} \times T^{3.25}\ \mathrm{Exp}\left(\frac{-5590\ \mathrm{cal/mol}}{RT}\right)\ \mathrm{cm^3\ mol^{-1}\ s^{-1}}$ as prescribed by Seta et al. [62], respectively for the analogous reactions of the toluene system.

3.3.4. Dimethyl benzyl radical reaction

The associated products of the hydrogen abstraction reactions are the 3,5-dimethylbenzyl radical and the 1,3,5-trimethylphenyl radical, Fig. 1. Using *ab initio* computational methods, Da Silva et al. [63] recently studied the decomposition of the meta-methylbenzyl (3-methylbenzyl) radical, the analogous radical formed from hydrogen abstraction from m-xylene. Da Silva et al. performed quantum chemical calculations at the G3SX(MP3)//B3LYP/6-31*G*(2*df*,*p*) level of theory that, through a complicated multistep reaction mechanism, suggest that para-xylylene (Fig. 1) + H atom are the major decomposition products of that radical. Thus in the present study the analogous, 3,5-dimethylbenzyl radical is assumed to decompose to release a H atom and the analogous closed shell product (to para-xylylene) at the high pressure limit rate constant proposed by Da Silva et al. for the overall m-methylbenzyl decomposition reaction, $3.26 \times 10^{13} \times T^{0.128}\ \mathrm{Exp}\left(\frac{-70.300\ \mathrm{cal/mol}}{RT}\right)\ \mathrm{cm^3\ mol^{-1}\ s^{-1}}$. The oxidation of the subsequent methyl xylylene is described by the adopted submodel of Gail et al. [25] previously proposed in their m-xylene oxidation study.

Bimolecular reaction of the 3,5-dimethylbenzyl radical with O atom and the HO_2 radical are also considered by direct analogy to the equivalent reactions of the benzyl radical of the toluene system [21]. Similarly, various radical recombinations are also considered including the reaction of two 3,5-dimethylbenzyl radicals to form the bibenzyl analogue at a rate constant of $5.0 \times 10^{12} \times T^{0.0}$ - $\times\ \mathrm{Exp}\left(\frac{-454\ \mathrm{cal/mol}}{RT}\right)\ \mathrm{cm^3\ mol^{-1}\ s^{-1}}$.

3.3.5. Reactions of other methyl substituted aromatic species

Finally, the work of Lifshitz et al. [64] on the aromatic ring expansion in methylcyclopentadiene (production of C_6 aromatic rings) has been adopted and additional analogous chemistry considered to describe the relevant species formed in the 1,3,5-trimethylbenzene and m-xylene submodels.

The resulting detailed model consists of 454 discrete chemical species participating in 2567 reactions. The base toluene model considers 329 species and 1888 reactions [21].

3.4. Reduced model

In order to test the model against the diffusion and premixed flame extinction data of Won et al. [31], Ji et al. [32], and Hui et al. [34] a large series (hundreds) of one dimensional diffusion flames of varying strain rate must be calculated in order to deduce the computed extinction condition. Thus necessarily, a reduced model for high-temperature flame conditions is produced from the detailed version by the mutli-generation path flux analysis method as implemented in the Princeton Chem-RC software [65]. The reduced model consists of 161 species and 1040 reactions. The necessary testing of this model has been performed, computations at temperatures greater than 1200 K compare closely against

those of the detailed model for selected test cases. All other computations utilise the detailed model. The detailed and reduced models are available in chemkin format as Supplemental material.

3.5. Model computations

Model computations are performed with the *chemkin solver* [66]. Shock tube simulations are performed with the *senkin* code exercised under constant volume, constant internal energy assumptions with the reflected shock temperature and pressure inputted as the initial conditions. The *senkin* code, under constant pressure constant internal energy assumptions is also utilised for simulation of the flow reactor scenarios. Flow reactor simulations were halted at the experimentally specified residence time, no manipulation of the physical gas residence time was used in comparing model computation to experiment [67]. The *premix* code is utilised to compute freely propagating flames from which the computed laminar burning velocity is determined. Grid sizes of approximately 1000 points, allowing increments of CURV and GRAD of 0.02–0.01 to be met, ensured grid independent solutions. Diffusion flame extinction limits are computed with the *oppdif* code following the procedure described by Won et al. [31] which utilises the reduced kinetic model and a plug-flow velocity profile. Multicomponent and thermal diffusive effects are considered in all of the transport coupled computations.

4. Results and discussion

4.1. Ignition delay

Ignition delay times for 1,3,5-trimethylbenzene/air mixtures are measured at three equivalence ratios (0.5, 1.0, and 2.0) at pressures of ~10 and ~20 atm in the 1111–1468 K temperature range, Table 1. The obtained ignition delay data are presented in Table 2 and compared to model computed ignition delays in Fig. 2.

Experiments show 1,3,5-timethylbenzene ignition delay to exhibit an Arrhenius-like temperature dependence, at all conditions studied. As one would expect the ignition delay also becomes shorter as pressure and/or the equivalence ratio is increased. A weak dependence on the equivalence ratio is observed between the fuel-lean ($\Phi = 0.5$) and stoichiometric mixtures ($\Phi = 1$), whereas the ignition delays of the fuel-rich mixture ($\Phi = 2$) are significantly shorter, approximately a factor of two at the lowest temperatures investigated. This behaviour is generally consistent with that of toluene ignition [21] and with a previous study of the xylene isomers [29].

From Fig. 2 it can be seen that the model successfully captures the trend in experimental observations for the fuel-lean and stoichiometric mixtures, including the influence of pressure. As observed experimentally, a modest dependence on equivalence ratio is computed by the model between the $\Phi = 0.5$ and $\Phi = 1$ mixtures relative to that computed for the $\Phi = 2$ mixture. However, the model underestimates the fuel reactivity in fuel-rich conditions at the lowest temperatures, with the largest experiment-model deviation a factor of 1.5.

Miyama [68] has previously determined similar reflected shock high temperature (1235–1925 K) ignition delays of a series of aromatic hydrocarbons at ~4–6 atm. Three compositions of 1,3,5-trimethylbenzene in O_2/Ar were studied, however only an empirical relation for the dependence of ignition delay on oxygen concentration and reflected shock temperature was provided,

$$\log t[O_2] = (12,200 \pm 530)/T - (8.72 \pm 0.23) \quad (1)$$

where t (μs) is the ignition delay time and T (K) the reflected shock temperature. The ignition delays computed by the kinetic model

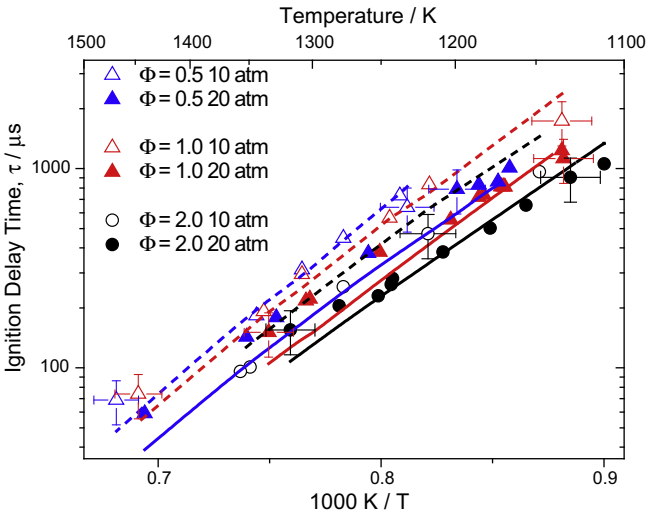

Fig. 2. Measured (symbols) and computed (lines) reflected shock ignition delays for 1,3,5-trimethylbenzene/air mixtures. Hollow symbols and dashed lines are ~10 atm conditions, solid symbols and solid lines are ~20 atm conditions.

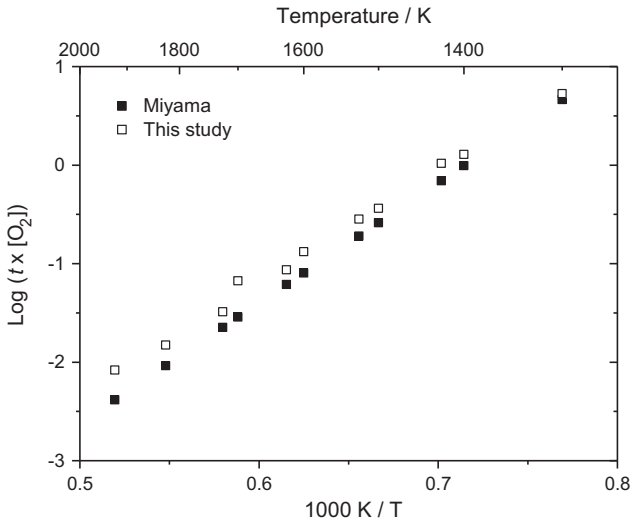

Fig. 3. Model comparison to the 1,3,5-trimethylbenzene shock tube ignition delay (τ) study of Miyama [68] at 4–6 atm. Solid symbols are derived from the experimental expression of Miyama, hollow symbols are kinetic model computations, see text.

proposed in this work when exercised at the conditions of Miyama may be fit to the similar relationship as,

$$\log t[O_2] = (11,419 \pm 243)/T - (8.11 \pm 0.16) \quad (2)$$

These data are graphically presented in Fig. 3 where the temperature intervals have been assumed. It is noted that the model computations of the Miyama conditions are also somewhat slower than experiment. The similarity in fitted parameters is a further indication of the performance of the model at high-temperature conditions.

4.2. Laminar burning velocity

Laminar burning velocities of 1,3,5-trimethylbenzene/air mixtures are measured at 400 K and 1 atm as a function of equivalence ratio, always in air, in increments of 0.1. The experimental data are

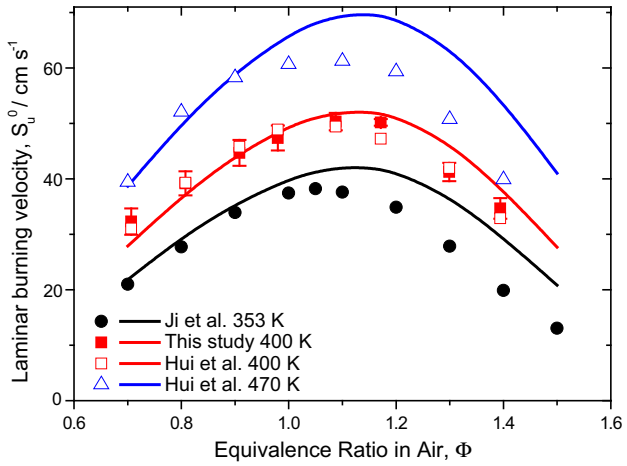

Fig. 4. Laminar burning velocities of 1,3,5-trimethylbenzene/air mixtures at 1 atm. Symbols are experimental data [32,34] and lines are model computations.

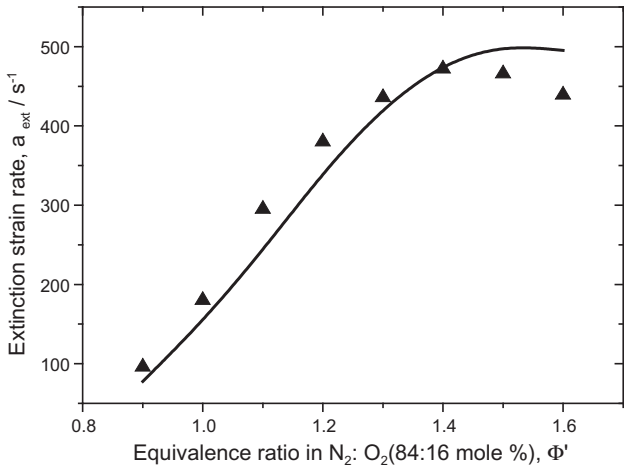

Fig. 6. Premixed counter-flow flame extinction strain rates of 1,3,5-trimethylbenzene in N_2:O_2 (84:16 mole%) at atmospheric pressure. Symbols are experimental data [34] and line model computations.

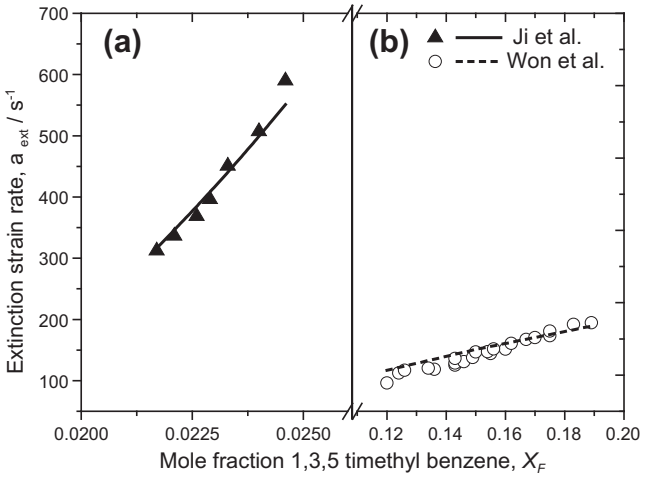

Fig. 5. Diffusion flame extinction strain rates of 1,3,5-trimethylbenzene/N_2 in counter-flow against (a) oxygen (Ji et al., 298 K [32], hollow symbols) and (b) air (Won et al., 300 K [31], solid symbols) at atmospheric pressure. Symbols are experimental data and lines are model computations.

presented in Fig. 4 with the previous measurements of Ji et al. [32] at the lower temperature of 353 K and those of Hui et al. [34] at temperatures of 400 K and 470 K, all also at 1 atm. The measurements reported in this study are in close agreement (within ~4%) with the measurements of Hui et al. for the same initial unburned gas temperature. The close agreement provides some confidence in the accuracy of the reported values as Hui et al. used the entirely different counter-flow flame technique, rather than the outwardly propagating flame technique as used in this study. The laminar flame speed exhibits a maximum value (S_L = 50.3 cm s^{-1}) at an equivalence ratio (Φ) of 1.1, in apparent agreement with the earlier measurements of Ji et al. [32] at the lower initial temperature of 353 K, who located the maximum burning velocity at an equivalence ratio of ~1.05, also consistent with the observations of Hui et al. [34] at 470 K (Φ = 1.10).

Model computations are also presented in Fig. 4, as lines. The model reproduces the majority of the experimental measurements for the highest temperature (470 K), but overestimates the flame velocities of the most fuel-rich mixtures (high equivalence ratios). The performance is similar against the 353 K data set of Ji et al. and both 400 K data sets, where the fuel lean, low equivalence ratio measurements are reproduced, but the model shows a disparity in computation of the more fuel rich mixtures. It should be noted that both Ji et al. and Hui et al. used a counterflow flame configuration of fuel/air pre-mixtures whereas the present work is performed with spherically propagating flames. For both techniques, the determination of the unstretched laminar flame velocity relies on an extrapolation to the zero stretch condition. The discrepancy in computations of all of the fuel rich data may include uncertainties due to the extrapolation techniques in addition to the definite uncertainties in chemical reaction pathway and rate constant parameters of the kinetic model.

4.3. Extinction limits

Won et al. [21] report the extinction limits of 1,3,5-trimethylbenzene/air diffusion flames measured in a counter-flow flame at atmospheric pressure, for initial fuel and oxidizer temperatures of 500 K and 300 K, respectively. Comparison of model computations to measurements of this combustion phenomena are provided in Fig. 5. The experimental measurements are reproduced by the model to within a precision of less than 5%. For convenience, the similar measurements of Ji et al. [32] are also plotted in Fig. 5 with model computations. It is noted than the measurements of Ji et al. and Won et al., though phenomenologically similar, are not comparable as the experimental conditions (temperature) and configuration (oxidizer composition) differ, no comparison is suggested. The model performance is similarly precise at the conditions of Ji et al. However, at both diffusion flame conditions the model is observed to compute a higher reactivity than observed in experiment. This is also the situation against the more fuel rich (Φ = 1.1–1.5) burning velocity cases. However, the model reproduces quite well the premixed extinction measurements of Hui et al. [34] as shown in Fig. 6.

4.4. Flow reactor

The oxidation of a dilute mixture of 1,3,5-trimethylbenzene/oxygen in nitrogen is studied at temperatures of 650–970 K at 12.5 atm for a residence time of 1.8 s in each case. From Fig. 7, no low-temperature reactivity is observed. The onset of reactant consumption and product formation occurs in a gradual manner, becoming appreciable at approximately 850 K. This indicates that

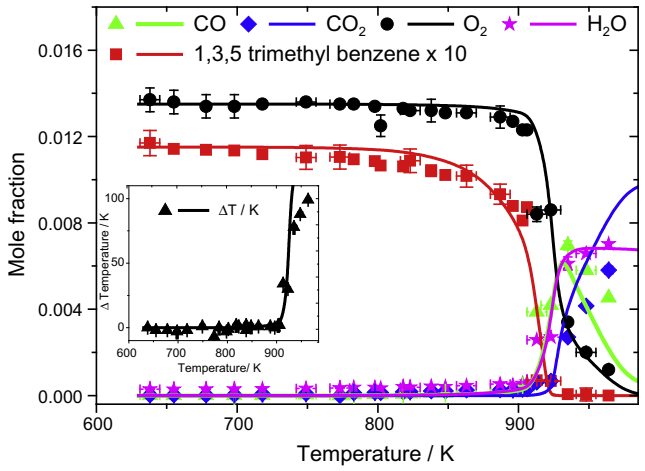

Fig. 7. Flow reactor oxidation data for conditions of 12.5 atm, 0.1111 mole% 1,3,5-trimethylbenzene in N_2, $\Phi = 1$ at 1.8 s residence time. Inset: heat release due to chemical reaction (ΔT). Symbols are experimental data and lines are model computations.

the degree of alkylation (methylation) to the aromatic ring is insufficient to support radical chain branching due to isomerization of any alkylperoxy radicals that may be formed. These experimental conditions are consistent with previous studies on jet-fuels [5,7], jet-fuel surrogates [5–7] and their constituent aromatic molecules [21], where 1,3,5-trimethylbenzene is observed to be much less reactive than jet fuel and its surrogates, but within experimental precision, approximately as reactive as toluene at similar conditions [21].

A principal purpose of this study is to allow for the development of a combustion model for jet aviation fuel by modelling an n-dodecane/iso-octane/n-propylbenzene/1,3,5-trimethylbenzene surrogate formulation which was shown in [6] to quantitatively emulate the detailed combustion performance of the specific real life aviation fuel it was formulated to mimic. Thus, it is satisfactory as an initial position that the kinetic model computations reproduce the general reactivity observed in experiment as indicated by the global combustion metrics of reactants, products and heat release apparent from Fig. 7.

The modelling prescriptions made in this study largely originate from detailed experimental and computational chemistry studies of the smaller but thermochemically similar toluene system, as summarised in [21]. Such dedicated studies of 1,3,5-trimethylbenzene are presently scarce [43–50] amounting to much less than the extensive knowledge base available for toluene oxidation/pyrolysis. The similarity in the model computations with experiment as shown in this study indicate that the approach is adequate to describe the overall rate of the global chemical reaction to a useful level of fidelity. However there is very limited information available with which to test the chemical mechanism that results from the sum of the thermochemical parameters, elementary reactions and rate constants prescribed from what is known to be true for the case of toluene oxidation. For the purposes of discussion, the chemical mechanism proposed by the model for the combustion of 1,3,5-trimethylbenzene is elucidated by rate of production analyses of the chemistry occurring under each kinetic environment of the different combustion scenarios studied.

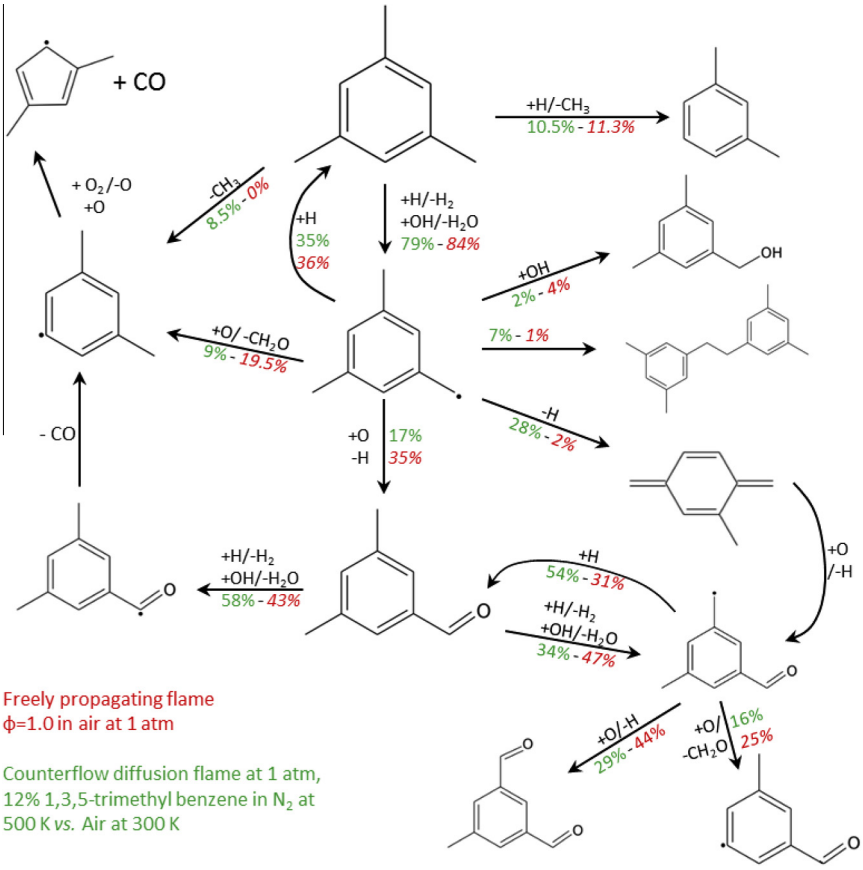

Fig. 8. Rate of production analysis of 1,3,5-trimethylbenzene oxidation in premixed freely propagating (red) and counter-flow diffusion (green) flames at atmospheric pressure. See text for details of flame configurations. (For interpretation of the references to colour in this figure legend, the reader is referred to the web version of this article.)

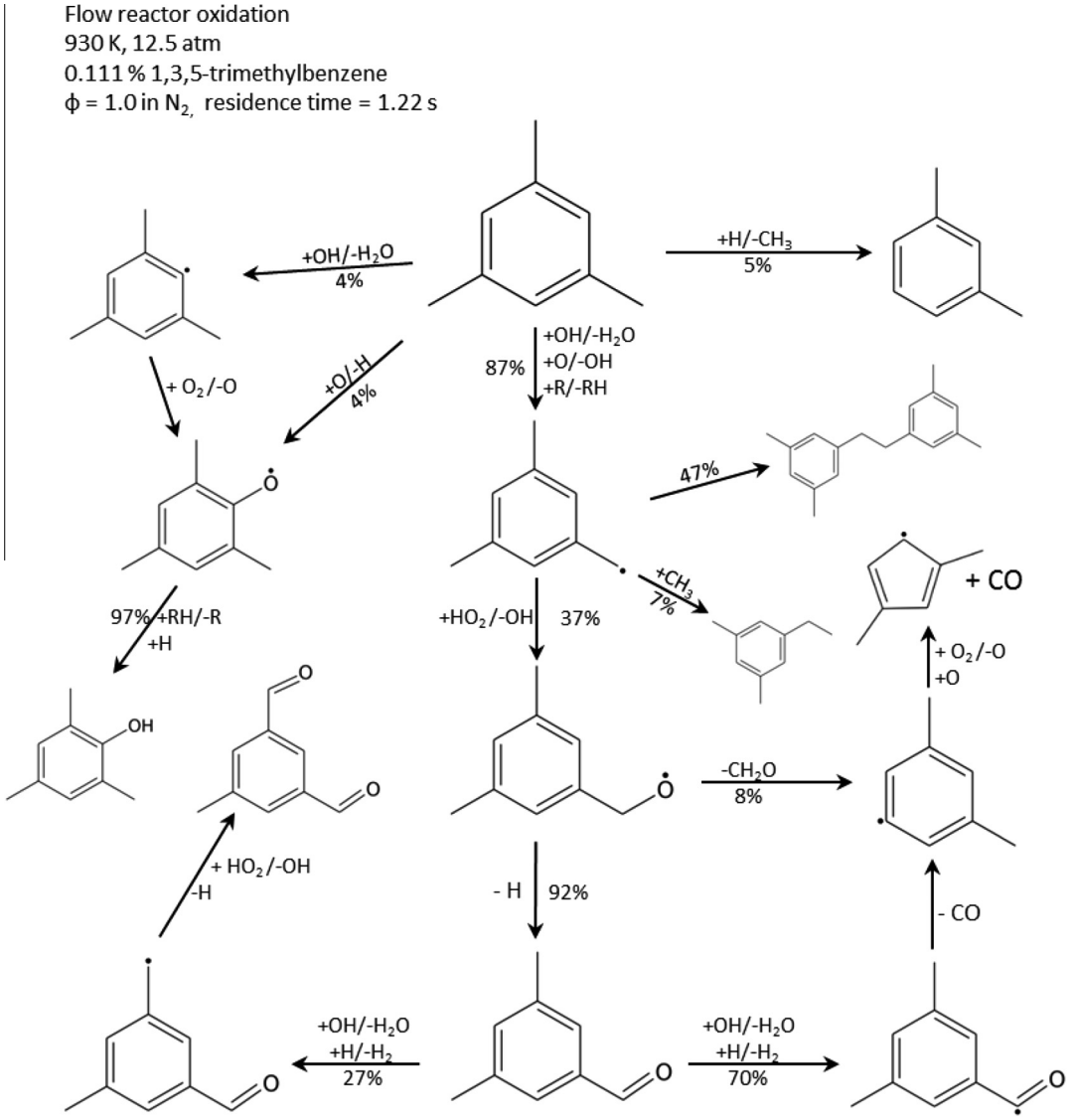

Fig. 9. Rate of production analysis of 1,3,5-trimethylbenzene oxidation at 50% 1,3,5-trimethylbenzene consumption at flow reactor conditions of are 0.1111% 1,3,5-trimethylbenzene, Φ = 1.023, 12.5 atm, and 930 K.

5. Reaction pathway analysis

5.1. Premixed and diffusion flames

The rates of the respective reaction pathways responsible for consumption of 1,3,5-trimethylbenzene have been integrated across the entire spatial domain of each flame. In general, analysis of the model computations shows that the same processes are responsible for consumption of the fuel in each flame, thus Fig. 8 presents results for representative premixed (stoichiometric freely propagating fuel/air flame at 1 atm and 400 K) and diffusion (12% fuel in N_2 at 500 K in counter-flow with air at 300 K at 1 atm, strain rate of 105 s^{-1}) flame configurations. The model suggests that the consumption of 1,3,5-trimethylbenzene mainly proceeds through the abstraction of a benzylic H atom to generate 3,5-dimethylbenzyl radicals. At the temperatures and diffusive environments of these flames, hydrogen atoms dominate as the abstracting species (accounting for 56% and 66% of 1,3,5-trimethylbenzene consumption in the analysed diffusion and premixed flames respectively), followed by OH radical at 12% and 27% respectively. A minor consumption channel ($\sim$ 10%) of the parent fuel is the displacement of a methyl group by a hydrogen atom to generate m-xylene and a methyl radical. Abstraction reactions of a hydrogen atom from the aromatic ring do not contribute significantly to the depletion of the initial fuel fraction.

From Fig. 8, at both conditions, a significant portion of the 3,5-dimethylbenzyl radicals formed, recombine with H atoms to regenerate 1,3,5-trimethylbenzene, respectively 35% and 36% of total 3,5-dimethylbenzyl radical consumption in the diffusion and premixed flames. However, the model does suggest a difference in the consumption of the remaining benzylic type radicals between premixed and diffusion flame configurations. In the premixed flame, the radical reacts with O atoms to generate 3,5-dimethylbenzaldehyde ($C_9H_{10}O$) (35%), and to a lesser extent (19.5%) 1,3-dimethylphenyl radicals (C_8H_9). In contrast in the diffusion flame scenario (uni) molecular decomposition producing an H atom and a methylxylylene (C_9H_{10}) molecule dominates, Fig. 7. Further oxidation of methylxylylene by O atoms results in the formation of 3,5-dimethylbenzaldehyde by H abstraction from either the carbonyl position or a methyl group. The resulting radicals then react by releasing either carbon monoxide and a dimethylphenyl radical or methyltolualdehyde respectively. The xylyl

radicals produced throughout the oxidation of 1,3,5-trimethylbenzene generate dimethylphenoxy radicals by reaction with molecular oxygen and further decomposition to carbon monoxide and a dimethylcyclopentadienyl radical.

The overall rate of oxidation of 1,3,5-trimethylbenzene in each flame is controlled by hydrogen-abstraction reactions of H atoms and the subsequent further oxidation of the radicals formed by O atoms. Oxygen atom is mainly (90%) produced through the radical chain branching reaction of H + O_2 = O + OH, and to a lesser extent through reactions specific to aromatic species. Thus the balance between H atom consumption by reaction with aromatic moieties or reaction with molecular oxygen is very important to the reactivity of the flame systems.

At these conditions, the model shows the radical–radical reaction involving HO_2 and the benzyl type radical to be inactive, presumably due to the low population of HO_2 at these atmospheric pressure conditions. As discussed below, this is not the case at the lower temperature, higher pressure flow reactor conditions.

In summary, the mechanism of 1,3,5-trimethylbenzene oxidation at flame conditions is generally bimolecular. This is distinct from the analysis presented by Hui et al. and Won et al. for similar flames of the isomeric, n-alkylated, n-propyl benzene, where a significant portion of that fuel was suggested to react by unimolecular decomposition.

5.2. Flow reactor oxidation

A rate of production analysis is conducted at flow reactor conditions of 0.1111% 1,3,5-trimethylbenzene in N_2, Φ = 1, 930 K, 12.5 atm and 50% 1,3,5-trimethylbenzene conversion, corresponding to a residence time of 1.22 s, i.e. the conditions of Fig. 7. The results are displayed in Fig. 9. As in the flame configurations, 1,3,5-trimethylbenzene reacts through H-abstraction reactions to produce the benzylic type radical. However in contrast to the flame environments the main abstracting species is the OH radical (accounting for 60% of total consumption). The resulting 3,5-dimethylbenzyl radicals undergo a significant amount of recombination to produce the diaromatic adduct (1,2-bis(3,5-dimethyl phenyl)ethane, 47%). The model shows that the consumption of the remaining 3,5-dimethylbenzyl radicals react with HO_2 to produce dimethylbenzoxy radicals (37%) and an OH radical.

At the high pressure and low temperature flow reactor conditions, the oxidation of 1,3,5-trimethylbenzene is governed by OH/HO_2 oxidation chemistry. HO_2 radicals are primarily produced by the reaction of H + O_2 (+M) = HO_2 (+M) (51%) and by the oxidation of the diaromatic adduct (22%). By comparison, the consumption of HO_2 is much more diverse, though it is noteworthy that more than 90% of the HO_2 radical consumption is from reaction with various aromatic species. Among these reactions, 41% of HO_2 is converted to an OH radical by reaction with the 3,5-dimethylbenzyl radical. This is an analogous process to that which is accepted to be a governing process in toluene oxidation and this reaction significantly (positively) influences the overall reactivity of the system.

5.3. Shock tube ignition delay

The chemistry accounting for the consumption of 1,3,5-trimethylbenzene under the conditions of the shock tube study is similarly analysed for the stoichiometric fuel-in-air mixture, (Mixture #1, Table 1) at 1304 K and 20.4 atm, as an example. Fig. 10 depicts the model analysis where the chemical flux is integrated over the entire temporal domain of the induction period. In general, the mechanism of oxidation at the higher temperature shock tube condition is very similar to that at the lower temperature (920 K) flow

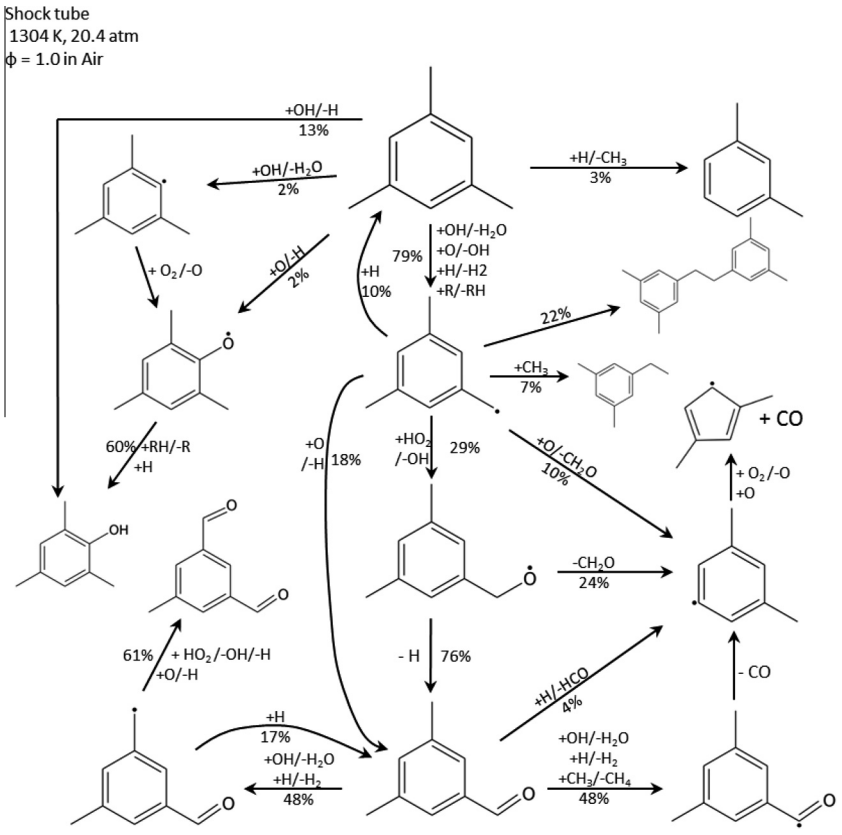

Fig. 10. Rate of production analysis for 1,3,5-trimethylbenzene oxidation in shock tube ignition delay at reflected shock conditions of fuel/oxygen/nitrogen 0.0187/0.2061/0.7752 (mole fraction), Φ = 1.0, 20.4 atm, and 1304 K.

reactor condition described above. Thus this discussion shall be limited to the major differences between each condition.

The major route of fuel consumption is again by hydrogen abstraction from the methyl position accounting for 79% of total. At ~1300 K, the H atom population is much higher than at 920 K, thus H atom appears as a major abstracting species. The consumption of the 3,5-dimethylbenzyl radical again proceeds by bimolecular reaction, principally with HO_2 radical and O atom, eventually resulting in the production of 3,5-dimethylbenzaldehyde. The model suggests the reaction flux through the diaromatic adduct, 1,2-bis(3,5-dimethyl phenyl)ethane, to be reduced relative to the flow reactor condition. However the model still suggests this species with 3,5-dimethylbenzaldehyde, to be the highest concentration stable intermediate species of mechanistic significance, together with toluene, benzene, acetylene, ethylene and methane as the other major intermediate hydrocarbon molecules during the 1,3,5-trimethylbenzene induction period.

6. Conclusions

Select combustion properties of 1,3,5-trimethylbenzene are measured at a range of combustion conditions in different experimental configurations that encompass both homogeneous and diffusively coupled reacting environments. Constant residence time flow reactor oxidative reactivity measurements show this trimethylated aromatic not to exhibit the low temperature reactivity typical of the alkylperoxy radical initiated low temperature chain branching mechanism. Reflected shock ignition delay measurements of 1,3,5-trimethylbenzene/air mixtures show the ignition delay time to decrease with increased equivalence ratio, temperature and pressure. Both behaviours are phenomenologically consistent with similar observations from toluene combustion [21]. The laminar burning velocity of 1,3,5-trimethylbenzene/air freely propagating flames have also been measured and share close agreement to those measured by Hui et al. [34] in the counter-flow flame configuration.

In order to facilitate the numerical modelling of high molecular weight real transportation fuels through the surrogate fuel concept, a chemical kinetic model is constructed for the global combustion behaviour of 1,3,5-trimethylbenzene. It is demonstrated that 1,3,5-trimethylbenzene exhibits a thermochemical environment similar to that of toluene. Given the paucity of data on the elementary oxidation reaction kinetics for 1,3,5-trimethylbenzene, this thermochemical similarity is utilised to prescribe the oxidation mechanism and reaction rate constants by analogy to the much better understood toluene system. Without any arbitrary adjustment, the model parameters reasonably reproduce the global combustion reactivity measurements described above, including observable trends with mixture composition and experimental condition. In the worst case, ignition delays are reproduced to within a factor of 1.8, laminar burning velocities are reproduced to within a factor of 1.19, and flow reactor reactivity to within ~15–20 K. In addition the calculations of the kinetic model also reproduce the suitable data available in the literature to a precision of 60% for laminar burning velocity, ~11% for premixed and diffusive extinction limits, and (negative) ~17% for premixed extinction limits.

The 1,3,5-trimethylbenzene oxidation mechanism that results from the modelling prescriptions is analysed at conditions representative of each of the combustion phenomena measured. At all conditions, it is suggested that 1,3,5-trimethylbenzene combustion occurs principally by hydrogen abstraction from a methyl position to yield the 3,5-dimethylbenzyl radical which reacts bimolecularly, depending on condition, to form 3,5-dimethylbenzaldehyde and 1,2-bis(3,5-dimethylphenyl)ethane as the major stable intermediate species of mechanistic significance. The combustion process is suggested to be driven through H/O atom reactions with 1,3,5-trimethylbenzene in flame configurations, whereas OH/HO_2 radical reactions drive 1,3,5-trimethylbenzene reactivity at lower temperatures. While the chemical mechanism of 1,3,5-trimethylbenzene combustion suggested by the kinetic model is sufficient to reproduce the global measurements reported here to the accuracies stated above, to further improve the fidelity of the kinetic model, detailed information of a mechanistic nature is required.

Acknowledgments

Work at Princeton University and Rensselaer Polytechnic Institute is supported by the Air Force Office of Scientific Research (AFOSR) under Grant No. FA9550-07-1-0515. and Grant No. FA9550-11-1-0261 respectively with Dr. Chiping Li and Dr. Julian Tishkoff (retired) as technical monitors. Work at University of Limerick is supported by Science Foundation Ireland under Grant No: 06/CP/E007.

Appendix A. Supplementary material

Supplementary data associated with this article can be found, in the online version, at http://dx.doi.org/10.1016/j.fuel.2012.11.069.

References

[1] Vanhove G, Petit G, Minetti R. Combust Flame 2006;145:521–32.
[2] Andrae JCG. Fuel 2008;87:2013–22.
[3] Pitz WJ, Cernansky NP, Dryer FL, Egolfopoulos FN, Farrell JT, Friend DG, Pitsch H. SAE paper 2007-01-0175; 2007.
[4] Violi A, Yan S, Eddings EG, Sarofim AF, Granata S, Faravelli T, et al. Combust Sci Technol 2002;174:399–417.
[5] Dooley S, Won SH, Chaos M, Heyne J, Ju Y, Dryer FL, et al. Combust Flame 2010;157:2333–9.
[6] Dooley S, Won SH, Heyne J, Farouk TI, Ju Y, Dryer FL, et al. Combust Flame 2012;159:1444–66.
[7] Dooley S, Won SH, Jahangirian S, Ju Y, Dryer FL, Wang H, et al. Combust Flame 2012;159:3014–20.
[8] Brezinsky K, Litzinger TA, Glassman I. Int J Chem Kinet 1984;16:1053–74.
[9] Klotz SD, Brezinsky K, Glassman I. Proc Combust Inst 1998;27:337–44.
[10] Dagaut P, Pengloan G, Ristori A. Phys Chem Chem Phys 2002;4:1846–54.
[11] Burcat A, Snyder C, Brabbs T. NASA TM 87312. Washington, DC: National Aeronautics and Space Administration (NASA); May 1986.
[12] Davidson DF, Gauthier BM, Hanson RK. Proc Combust Inst 2005;30:1175–82.
[13] Vasu S, Davidson DF, Hanson RK. J Propul Power 2010;26:776–83.
[14] Sakai Y, Inamura T, Ogura T, Koshi M, Pitz WJ. SAE [Tech Pap]; 2007 [10.4271/2007-01-1885].
[15] Shen H-PS, Vanderover J, Oehlschlaeger MA. Proc Combust Inst 2009;32:165–72.
[16] Sivaramakrishnan R, Tranter RS, Brezinsky K. Combust Flame 2004;139:340–50.
[17] Emdee JL, Brezinsky K, Glassman IJ. J Phys Chem 1992;96:2151–61.
[18] Da Costa I, Fournet R, Billaud F, Battin-Leclerc F. Int J Chem Kinet 2003;35:503–24.
[19] Klippenstein SJ, Harding LB, Georgievskii Y. Proc Combust Inst 2007;31:221–9.
[20] Oehlschlaeger MA, Davidson DF, Hanson RK. J Phys Chem A 2006;110:6649–53.
[21] Metcalfe WK, Dooley S, Dryer FL. Energy Fuels 2011;25:4915–36.
[22] Harding LB, Klippenstein SJ, Georgievskii Y. J Phys Chem A 2007;111:3789–801.
[23] Hippler H, Reihs C, Troe J. Proc Combust Inst 1991;23:37–43.
[24] Gaïl S, Dagaut P, Black G, Simmie JM. Combust Sci Technol 2008;180:1748–71.
[25] Gaïl S, Dagaut P. Combust Sci Technol 2007;179:813–44.
[26] Gaïl S, Dagaut P. Combust Flame 2005;141:281–97.
[27] Gudiyella S, Malewicki T, Comandini A, Brezinsky K. Combust Flame 2011;158:687–704.
[28] Battin-Leclerc F, Bounaceur R, Belmekki N, Glaude PA. Int J Chem Kinet 2006;38:284–302.
[29] Shen H-PS, Oehlschlaeger MA. Combust Flame 2009;156:1053–62.
[30] Roubaud A, Minetti R, Sochet LR. Combust Flame 2000;121:535–41.
[31] Won SH, Dooley S, Dryer FL, Ju Y. Proc Combust Inst 2011;33:1163–70.
[32] Ji C, Dames E, Wang H, Egolfopoulos FN. Combust Flame 2012;159:1070–81.
[33] Farrell JT, Johnson RJ, Androulakis IP. SAE paper 2004-01-2936; 2004.
[34] Hui X, Das AK, Kumar K, Sung C-J, Dooley S, Dryer FL. Fuel 2012;97:695–702.
[35] Honnet S, Seshadri K, Niemann U, Peters N. Proc Combust Inst 2009;32:485–92.
[36] Pitz WJ, Mueller CJ. Prog Energy Combust Sci 2011;37:330–50.

[37] Kim HH, Won SH, Santner J, Chen Z, Ju Y. Proc Combust Inst 2013;34:929–93.
[38] Qin X, Ju Y. Proc Combust Inst 2005;30:233–40.
[39] Chen Z. Studies on the initiation, propagation, and extinction of premixed flames. Ph.D. thesis, Princeton University; 2008.
[40] Chen Z, Burke MP, Ju Y. Combust Theory Model 2009;13:343–64.
[41] Held TJ, Dryer FL. Int J Chem Kinet 1998;30:805–30.
[42] Jahangirian S, Dooley S, Haas FM, Dryer FL. Combust Flame 2012;159:541–51.
[43] Perry RA, Atkinson R, Pitts Jr JN. J Phys Chem 1977;81:296–304.
[44] Ohta T, Ohyama T. Bull Chem Soc Jpn 1985;58:3029–30.
[45] Atkinson R, Aschmann SM. Int J Chem Kinet 1989;21:355–65.
[46] Kramp F, Paulson SE. J Phys Chem A 1998;102:2685–90.
[47] Tsang W, Cui JP, Walker JA. In: 17th Int Symp Shock Waves Shock Tubes, vol. 208; 1989. p. 63–73.
[48] Tsang W, Walker JA. J Phys Chem 1992;96:8378–84.
[49] Smith DF, Kleindienst TE, McIver CD. J Atmos Chem 1999;34:339–64.
[50] Aschmann SM, Long WD, Atkinson R. J Phys Chem A 2006;110:7393–400.
[51] Benson SW. In: Thermochemical kinetics. New York: Wiley; 1976.
[52] Orlov YD, Lavrov VO, Lebedev YA. Russ Chem Bull Int Ed 2001;50:96–969.
[53] Burcat A, Ruscic B. In: 3rd Millenium ideal gas and condensed phase thermochemical database for combustion with updates from active thermochemical tables, November 2011.
[54] Draeger JA. J Chem Therm 1985;17:263–75.
[55] Tee LS, Gotoh S, Stewart WE. I&EC Fundam 1966;5:356–63.
[56] Korean database, <http://www.cheric.org/kdb/>.
[57] Dooley S, Uddi M, Won SH, Dryer FL, Ju Y. Combust Flame 2012;159:541–51.
[58] Bounaceur R, Da Costa I, Fournet R, Billaud F, Battin-leclerc F. Int J Chem Kinet 2005;37:25–49.
[59] Chang AY, Bozzelli JW, Dean AM. Z Phys Chem 2000;214:1533–68.
[60] Sheng C, Bozzelli JW, Dean AM, Chang AY. J Phys Chem A 2002;106:7276–93.
[61] Ellis C, Scott MS, Walker RW. Combust Flame 2003;132:291–304.
[62] Seta T, Nakajima M, Miyoshi A. J Phys Chem A 2006;110:5081–90.
[63] da Silva G, Moore EE, Bozzelli JW. J Phys Chem A 2009;113:10264–78.
[64] Lifshitz A, Tamburu C, Suslenky A, Dubnikova F. Proc Combust Inst 2005;30:1039–47.
[65] Sun W, Chen Z, Gou X, Ju Y. Combust Flame 2010;157:1298–307.
[66] (a) R. J. Kee, G. Dixon-Lewis, J. Warnatz, M. E. Coltrin, J. A. Miller, Technical Report SAND86-8246, Sandia National Laboratories, Albuquerque, NM, 1986.(b) R. J. Kee, F. M. Rupley, E. Meeks, J. A. Miller, CHEMKIN-III: a FORTRAN chemical kinetics package for the analysis of gas phase chemical and plasma kinetics, SAND96-8216, Sandia Laboratories, 1996.
[67] Zhao Z, Chaos M, Kazakov A, Dryer FL. Int J Chem Kinet 2008;10:1–18.
[68] Miyama A. J Phys Chem 1971;75:1501–4.